Detection and Statistical Analysis of Human Cortical Sulci

Nicolas Royackkers, Michel Desvignes, Houssam Fawal, Marinette Revenu

Detection and statistical analysis of human cortical sulci

Nicolas Royackkers, Michel Desvignes, Houssam Fawal, Marinette Revenu

GREYC-ISMRA (UPRESA CNRS 6072)

6, Bd Maréchal Juin 14050 CAEN Cedex France

Tel: +33 2 31 45 27 01

Fax: +33 2 31 45 26 98

Email: Nicolas.Royackkers@greyc.ismra.fr, Michel.Desvignes@greyc.ismra.fr,

Marinette.Revenu@greyc.ismra.fr

Abstract

Many studies dealing with the human brain use the spatial coordinate system of brain anatomy to localize functional regions. Unfortunately, brain anatomy, and especially cortical sulci, are characterized by a high interindividual variability. Specific tools called anatomical atlases must then be considered to make the interpretation of anatomical examinations easier. The work described here first aims at building a numerical atlas of the main cortical sulci.

Our system is based on a database containing a collection of anatomical MRI of healthy volunteer brains. Their sulci have been manually drawn and labeled for both hemispheres. Sulci are represented as 3D superficial curves. After a non-linear registration process, a statistical atlas of the cortical topography of a particular MRI is built from the database. It is an a priori model of cortical sulci, including three major components: an average curve represents the average shape and position of each sulcus; a search area accounts for its spatial variation domain; a set of quantitative parameters describes the variability of sulci geometry and topology.

This atlas is completely individualized and adapted to the features of the brain under examination. The atlas is represented by a graph, the nodes of which represent sulci, and the edges the relations between sulci. It can also be considered as a statistical model that describes the cortical topography as well as its variability.

1. Introduction

Recent progress in the techniques of cerebral imaging are now allowing in vivo examination of both human cerebral anatomy (MRI, XCT) and cerebral functions (PET, EEG, MEG, fMRI). Such images are often interpreted in comparison to the brain of an ideal average patient, represented as a standard atlas. In vivo images and atlases can be used to identify and localize pathological areas as well as surgical paths leading to them, so as to minimize cortex or blood vessels lesions hazards and post-operation after-effects (Mangin et al. 1995). They can also help to get precise interpretation and correlation between cerebral anatomy and cerebral functions of the same subject or between several subjects. Pathology diagnosis can also be made easier by the study of the variations of cerebral structures that become abnormal under the effect of some disease (Thompson et al. 1996b).

The first paper atlases where built from a unique subject (Talairach and Tournoux 1988) or a few post-mortem brains (Ono et al. 1990). They constitute a unique reference system, where individual variations between real data and atlas data must be taken into account during the registration or interpretation process, which is usually performed by a specialist.

Digital atlases, based on the same principles as paper atlases, but inscribed on a numerical support, have led to the development of sophisticated registering methods between individual data and atlas data. Registration using the Talairach space is now widely adopted (Friston et al. 1995, Vérard et al. 1997). Non-linear methods allow a more accurate registration. They can be based on a manual process (Greitz et al. 1991), on elastic models (Bajscy and Kovacik 1989), or on fluid models (Christensen et al. 1995, Thompson and Toga 1996). However, in all previously mentioned methods, interindividual variability is taken into account by a registration process. The underlying assumption is that all human healthy brains can be compared to a single model (the atlas) that can be warped continuously, which seems unrealistic when considering the high structural variability of the cortex.

Another approach consists in including this variability into the atlas itself, so as to use it in the registration as well as in the interpretation process. It produces probabilistic atlases which are based on a model of the variability of points (Evans et al. 92), structures (Le Goualher et al. 1998, Mangin et al. 1995, Royackkers 1997) or deformations (Thompson et al. 1996a).

Our work belongs to the category of probabilistic atlases, but two kinds of brain anatomy variability are distinguished. Extrinsic variability (Steinmetz et al. 1989), due to the variability of global shape and size of the brain, can be reduced by means of a non-linear registration. Intrinsic residual variability, which accounts for local deformations specific to each subject, can then be modeled. This approach is used to automatically build an atlas of cortical sulci, with the goal to perform an automatic recognition of these sulci in other examinations. All necessary measurements on sulci are automatically computed from MRI, thus allowing the reproduction of the same process on further examinations. These measurements are adapted to each new examination, so as to take into account the anatomical variability of each subject. In our atlas, intrinsic variability is represented in a probabilistic way.

2. Materials and methods

2.1 Database

The atlas building uses a database that features:

- MRI examinations, containing images of human brain extracted from the head and orientated in the same standard way,
- for each brain, a set of coordinate completely defining the Talairach grid,
- For each one of the two hemispheres of each brain, labeled superficial curves representing the emerging part of a set of major cortical sulci.

These curves, which can be locally interrupted, are stored as ordered lists of points. Each point is defined by three integer coordinates in the discrete coordinate system of the image, and the local depth of the sulcus at this point (this depth is automatically computed).

2.1.1 MRI acquisition

43 anatomical MRI from different subjects are used in our work. These images were made from 1991 to 1997 at the Hospital of Caen ("CHRU de Caen"). They involve healthy volunteers including 19 men, 11 women and 13 subjects of unknown sex. The subjects whose age is known were from 20 to 54 years old, with an average age of 28 years and a standard deviation of 7 years.

Examinations are performed on a SIGNA 1.5T from General Electric. Most images are obtained with the same acquisition parameters. This 3D SPGR sequence produces 124 sagittal sections of the head, with a thickness of 1.3 mm and representing a 330 x 330 mm field of view in a 16-bit depth (1.3 mm^3 isotropic voxels). Other main parameters are: echo time (TE): 8 ms, repetition time (TR): 40 ms, flip angle (α): 45, total duration of examination: 16 min 27 s.

11 from the 43 available images are acquired with variations of the previously described acquisition sequence: 8 ones are composed of 1.5 mm^3 isotropic voxels, and 3 others are composed of axial sections. In all cases, MRI are T1-weighted 3D images with an optimized contrast between gray and white matter.

2.1.2 Brain extraction and orientation

The first goal is to separate the brain voxels from the rest of the head, and to get a standard orientation to the brain. This processing is performed by a software called "Atomia", which has been developed at the Cyceron center since 1991 (Quinton et al. 1997).

Orientating the brain is performed in two steps. The first one consists in detecting the interhemispheric plane, and then bringing it into alignment with the sagittal plane of the image by performing two rotations. The second step aims at defining an horizontal axis for the head thanks to two anatomical points belonging to the interhemispheric plane and called AC and PC. A rotation is then performed to align these points with the axial plane of the image. The head can thus be orientated in relation to the three major planes of the image. AC, PC and the interhemispheric plane define the Talairach coordinate system (or the Talairach grid) of the brain image. The brain can then

be extracted thanks to thresholding and mathematical morphology operators. A last operation consists in re-centering the extracted brain in the image (Vérard et al. 1997, Quinton et al. 1997).

2.1.3 Segmentation of sulci

Starting from a segmented and standard orientated brain, the aim is to automatically obtain the sulci as curves drawn on the surface of the hemispheres. It is achieved in three steps : thresholding, 3D skeletonization and superficial thinning (Fawal 1995).

2.1.3.1 Thresholding

An automatic thresholding based on the gray level histogram of the brain surface is first applied in order to obtain all the points of the brain belonging to sulci. This histogram analysis is performed separately for each hemisphere.

The gray level which shows the maximum frequency on the hemisphere surface is detected. This threshold allows to get a binary image where the darkest points correspond to the whole LCR and most of the gray matter (sulci points) and the brightest points correspond to the rest of the gray matter and the whole white matter.

Results are generally satisfactory : artificial interruptions or connections stay within an acceptable level, and the superficial aspect of the brain is consistent with the original brain image (see Figure 1 and Figure 3). Nevertheless, it can be necessary to manually correct the threshold in a few images, in order to avoid local sub-segmentation artifacts leading to the loss of significant parts of sulci or connections between sulci.

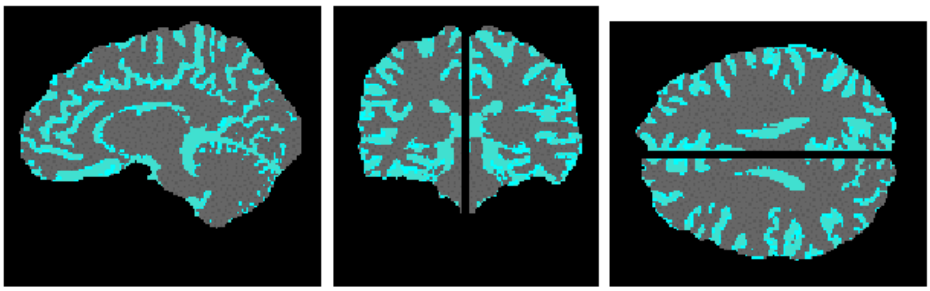

Figure 1 – Three sections of a cerebral volume after thresholding. From left to right : sagittal section, coronal section and axial section. Blue parts include sulci volume.

2.1.3.2 3D Skeletonization

A 3D skeletonization is achieved in order to transform sulci into thin surfaces representing their median part. Our skeletonization algorithm is adapted from the discrete skeletonization algorithm from Tsao and Fu (Tsao and Fu 1981), which is based on the local topology of objects. An exploration window is used (3 voxel-wide cube), where sulcus points are suppressed according to their neighborhood with other sulcus points included in the cube. This is successively applied across the whole image according to its six principal directions (north, south, east, west, bottom, top).

So as to be satisfactorily applied to the sulcus volume, the original skeletonization method had been modified. This modification concerns the object on which the skeletonization is applied. It consists in adding an imaginary voxel layer around the brain, which is not modified by the skeletonization process. Thus, one can get a sulcus skeleton that remains connected to the brain surface, instead of "sinking" into the brain because of the iterative suppression of superficial sulcus points. This is justified by the fact that we want to build a model of the superficial part of sulci only.

The result is a skeleton defined in 26-neighborhood, where each sulcus is represented as a thin surface. It is centered into the original sulcus volume and connected to the brain surface, as shown in Figure 2.

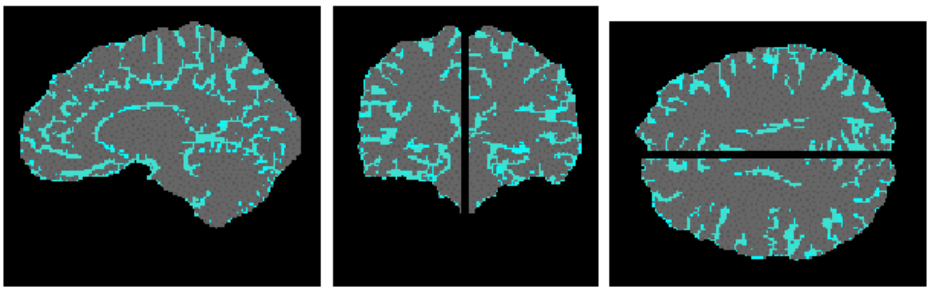

Figure 2 – Internal aspect of sulci after skeletonization.
These sections are the same as in Figure 1.

As mentioned before, superficial sulcus points are not modified by our skeletonization. Thus, sulci still appears as thick objects at the surface of the brain (Figure 3). Since we want to build a model of sulci represented as curves, a third processing step must take place.

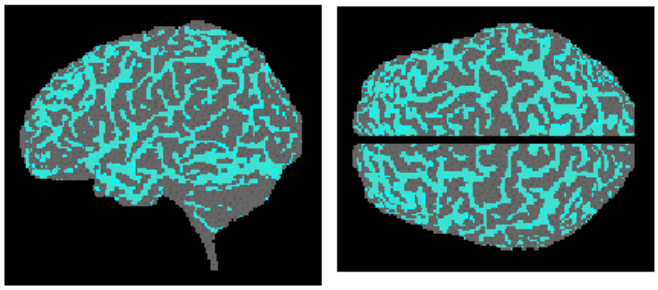

Figure 3 - External aspect of sulci. It is unchanged by skeletonization.

2.1.3.3 Superficial thinning

A superficial thinning process finally leads to the transformation of the superficial part of sulci into curves. This thinning is a 3D extension of a classical 2D thinning algorithm based on the Golay alphabet. It works with a 2D structuring element which is distorted so as to take into account the different surface shapes that may be contained into a 3 voxel-wide cube (exploration mask).

The thinning process is performed in an iterative way until sulci are no longer modified. At each iteration, the exploration mask is applied across the whole image according to its six principal directions. At each position of the mask, two 2D orthogonal projections that are parallel to the moving axis of the mask are considered. If the point located in the center of the cube both belongs

to sulci and to the brain surface, it can be removed according to the numerous rules adapted from the original 2D algorithm (Fawal et al. 1995).

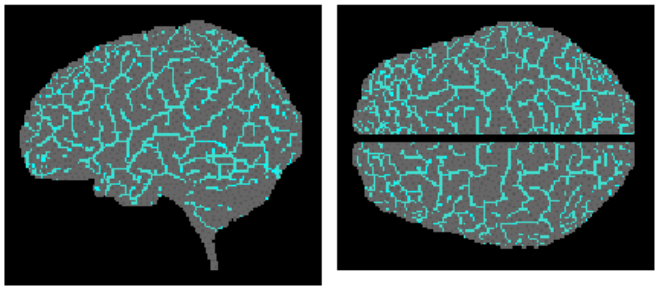

Figure 4 - External aspect of sulci after superficial thinning, in the same sections as in Figure 3.

After this three-step processing, sulci appear as thin surfaces into the brain and as an interconnected network of thin curves onto the hemispheric surface (Figure 5). These curves will form the basic primitives of our modeling process.

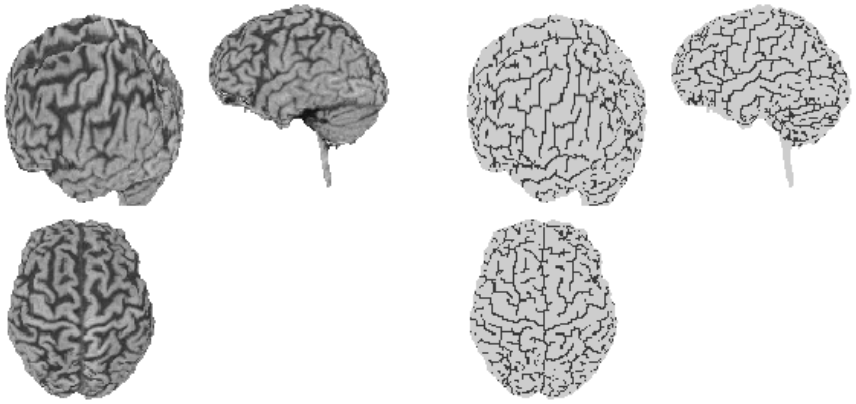

Figure 5 – Segmentation of sulci. On the left, the original brain MRI; on the right, sulcus points belonging to the surface of both hemispheres.

2.1.4 Depth computation

Our sulcus model concentrates on the superficial part of cortical sulci. It is a simple, natural and convenient means to represent sulci, since it is easier to draw, characterize and visualize a curve on the brain surface than the whole volume of a sulcus buried inside an hemisphere. The superficial part of sulci is also by far better known as it is more frequently studied and represented in atlases.

Nevertheless, only a small part of each sulcus is taken into account, and nothing in the parameters of a curve reveals anything about the buried sulcus it is connected to. So as to obtain information on the rest of each sulcus, and more particularly its penetration into the brain, a local depth associated to each point of the curve modeling the sulcus is computed.

The depth of a cortical fold must be computed from the thresholded image, since the dimensions of skeletonized objects are lower than those of the original ones. The local depth associated to a superficial point of a sulcus curve is defined as the distance between this point and the farthest sulcus point belonging to an orthogonal plan to the curve axis. The curve axis is defined as the tangent to the curve at the superficial point. The plan where the sulcus bottom is found is perpendicular to the axis and contains this superficial point.

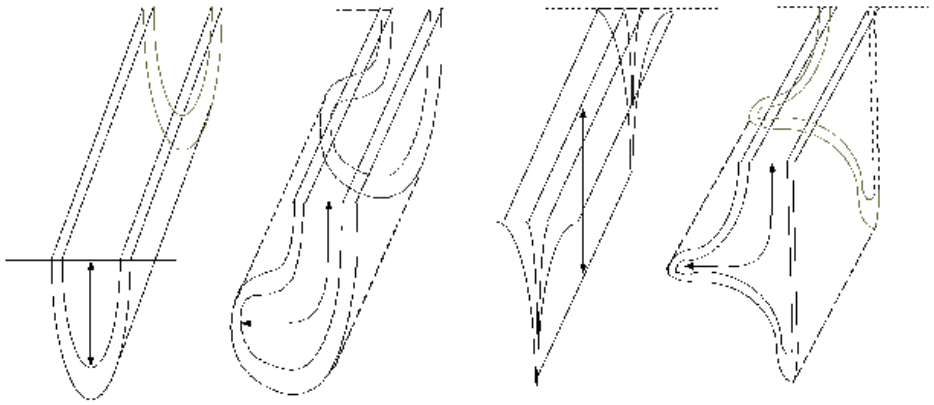

Figure 6 – Examples of possible shapes for a cortical sulcus.
For each shape, the arrow shows the depth that should be computed.

To compute the depth of a sulcus at a superficial point O, the local axis is first computed thanks to the examination of neighbor sulcus points in a 7 voxel-wide cube centered around point O. The theoretical equation of the plan P that is perpendicular to this local axis in O can then be easily obtained. The voxels belonging to the discrete corresponding plan are given by computing the intersection of P with the hemispheric points. Within this plan, two types of points can be found: sulcus points and non-sulcus ones. The set of sulcus points connected to O (in 26-neighborhood) is

then computed. The depth in O is the geodesic distance from O to the farthest point to O belonging to this set. In a case of a ramified sulcus, it is its longest branch which is thus measured (Desvignes et al. 1993).

Ours depth computation method gives good results. As described in section 3.1.1, computed average depths are generally very close to those given by neuroanatomical atlases. However, some local errors can be found along a sulcus. They are generally caused by an erroneous choice of the local curve axis, which leads to a depth computation in a misorientated plan. Such errors can frequently appear at the intersection of two sulci. They can also be due to brain segmentation problems (irregular hemisphere surface) or sulci segmentation problems (artificial connections or interruptions). Such local errors lead to discontinuities in the depth histogram along a sulcus, which can be eliminated by applying a median filtering (Figure 7).

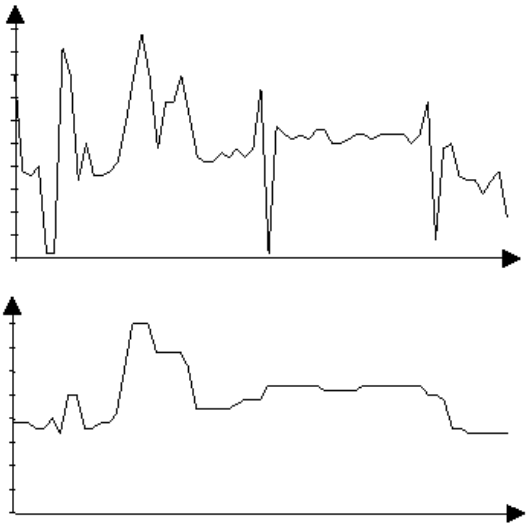

Figure 7 – An example of depth histograms obtained along a lateral sulcus : depth without filtering (top) and depth with filtering (bottom).

2.1.5 Building a graph of topological segments

The goal is here to structure the superficial curves network, until then considered as a set of indistinct points. A partition is performed to get a set of portions of these curves that will further be called "topological segments". All processing steps described in this section are completely automatic ones.

A topological segment is defined as a set of connected voxels joining two terminal points or nodes of the curves. A terminal point is an ending point of a curve: only one of its 26 neighbors belongs to the sulcus points. A node is a point where several curves are touching or crossing one another: at least three of its neighbors belong to the sulcus points.

The following of topological segments starts from a random point of the curve network. It consists in searching all segments that are connected to this starting point. In order to find the paths with the strongest connectivity between points, the following is successively performed in 6-neighborhood, 18-neighborhood and 26-neighbourhood. If the latter ends without having reached all sulcus points, then another following starts from a new starting point among those not encountered in the course of the previous followings.

To make sure that segments strictly adhere to the topological segment definition, the elements found after this following process are modified in several ways. Short terminal loops (a few points) are removed. In non terminal loops composed of two branches with the same starting point and the same ending point, the longer branch is suppressed. Non-looping segments connecting at a starting point which is not a node of the network are concatenated.

Finally, we get graph of topological segments. Each segment is a sequence of voxels connected by pairs and shares a unique label. It is arbitrarily orientated, with a starting point and an ending point (Figure 8).

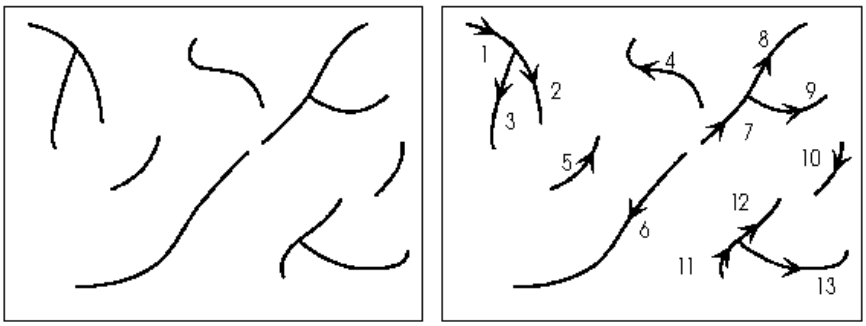

Figure 8 – Building the graph of topological segments.
On the left, a set of indistinct points composing a network of superficial curves.
On the right, the corresponding graph of labeled and orientated segments.

Typically, 250 to 350 topological segments can be found on the surface of each hemisphere. Their length varies from two to several tens of points. The superficial part of each cortical sulcus can be localized on a path composed of some of these segments.

2.1.6 Interactive designation of sulci

The superficial drawing of sulci and their labeling are performed by a neurosurgeon from the anatomy laboratory of the Hospital of Caen. This interactive identification is based on the commonly admitted anatomical nomenclature found in reference paper atlases (in particular, Damasio 1995 and Ono et al. 1990). The drawing work is performed with a graphical editor developed by our team. The curve representing each sulcus is manually built by successively pointing to the different topological segments which belongs to it. This process is performed so that the drawn sulcus may be as close as possible to the point-to-point manual drawing the expert would have done for the same sulcus, instead of pointing at successive curve portions coming from the segmentation described in sections 2.1.3 and 2.1.5.

First, sulci in 9 MR images were completely identified by our medical expert. The same will be done with the other available MRI as soon as possible. The authors, who are not medical experts, drew the sulci themselves in 19 other MRI with the help of several paper atlases (Damasio 1995, Ono et al. 1990, Talairach and Tournoux 1988).

This operation was necessary in order to obtain a large enough database to allow the evaluation of the developed tools within a reasonable time. The corresponding lines and the rules that guided their drawing has been verified in some MR examinations by a neuroradiologist from the MRI service of the Hospital of Caen. Finally, we get a database containing 28 images. 14 of them, randomly selected, will be used to build the sulci atlas. The other 14 will be used to test our automatic recognition method.

2.2 Building the atlas

All sulci of the database are registered in the same coordinate system (the choice of this coordinate system and the registration process will be discussed in section 2.3.1). They are used to build an atlas of the cortical topography. This a priori model of sulci geometry and topology is made of three components: an average curve, a search area, and a set of statistical data.

2.2.1 Average curve

The average curve is a unique curve obtained by geometrically averaging the set of curves representing the same sulcus in the different images of the database (Figure 9). It is an a priori model of the average shape and location of a sulcus. It also provides information on the local depth of the sulcus.

We have a set of curves C_i (with $i \in [1,n]$), which are n instances of the same sulcus from n different subjects. Each curve is defined by an ordered list of vectors $V_j=(x_{i,j},y_{i,j},z_{i,j},P_{i,j})$ (with $j \in [0,m_i]$). $x_{i,j}$, $y_{i,j}$ and $z_{i,j}$ are three integer coordinates defining point $M_{i,j}$ in the common coordinate system. $P_{i,j}$ is the local depth of the sulcus, expressed in millimeters. Let us now consider a parameter l in [0,1]. For any C_i curve, the V_k vector corresponding to the value l_0 of l is such that $k=\text{round}(m_i.l_0)$ (where round is the function that rounds a floating-point number to the nearest integer). For each value of l, we have one point for each curve, as well as one depth value. $B_l=(x_l,y_l,z_l)$ is defined as the center of gravity of the n points corresponding to the same l value, and P_l the average depth of these points. The C_m curve is defined by the ordered list of vectors $V_l=(x_l,y_l,z_l,P_l)$ for l varying continuously between 0 and 1.

Actually, the k parameter can be seen as a discrete curvilinear abscissa. Considering a broader definition of curves by $C_i(s)$ equations, the average curve $C_m(s)$ can finally be defined by the $M_m(s)$ points that verify: $\vec{OM}_m(s) = \frac{1}{n}\sum_{i=1}^{n} \vec{OM}_i(s)$.

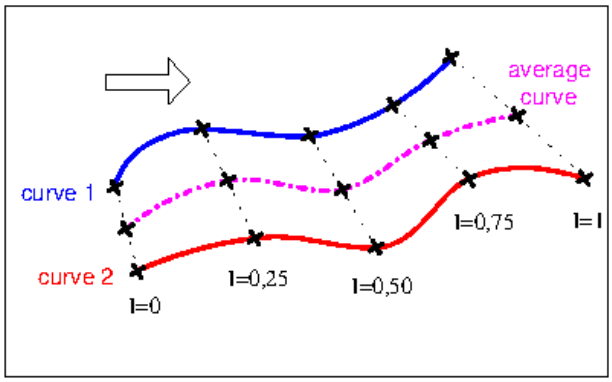

Figure 9 –Building the average curve from a set of sulci, illustrated here with two sulci described by the l parameter varying from 0 to 1.

Our method for building the average curve is easy and fast to perform. As Figure 10 shows, the results are satisfactory.

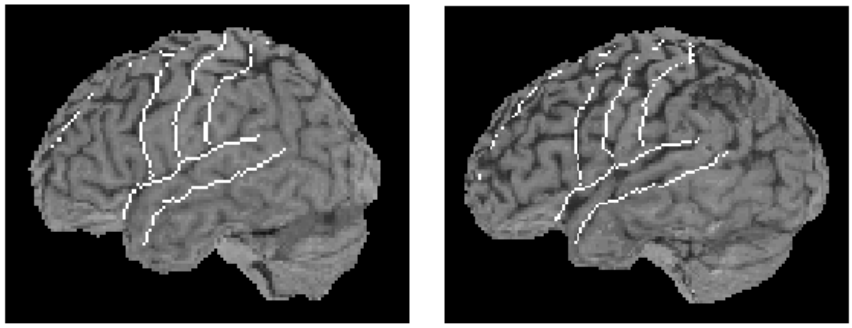

Figure 10 – Average curves in two different MRI (lateral projection of the left hemisphere).

2.2.2 Search area

The search area is a model of the variability of shape and position of a sulcus. It stems on the following idea: the definition of the search area for one given sulcus must be based on the location of instances of the same sulcus type identified in the database images. The area obtained by

registration in a common coordinate system of the curves corresponding to the same sulcus matches this definition. However, the resulting region has local holes, while its border is very indented.

So as to solve this problem, a first step consists in a geodesic dilatation of the region: a point of the hemispheric surface is added to the area if at least one of its 26-neighbors belongs to the initial region. This operation leads to the suppression of most holes, but also creates a one voxel wide "security margin" around the area. Actually, the addition of this margin is necessary because of the low number of images composing our database. With a larger database, one could also consider building a probabilistic sulcus location map, which would give useful information to a recognition process and prevent sensitivity to outliers of the search area building.

A second step aims at smoothing the border of the area so that it looks like the one which would have been obtained if it had been manually drawn around the original projected area. A conditional, geodesic and iterative dilatation is performed: at each iteration, a surface point is added to the region if at least four of its neighbors are already belonging to the region. The process stops when the number of added points at this step reaches the number of voxels added during the first geodesic dilation (Figure 11).

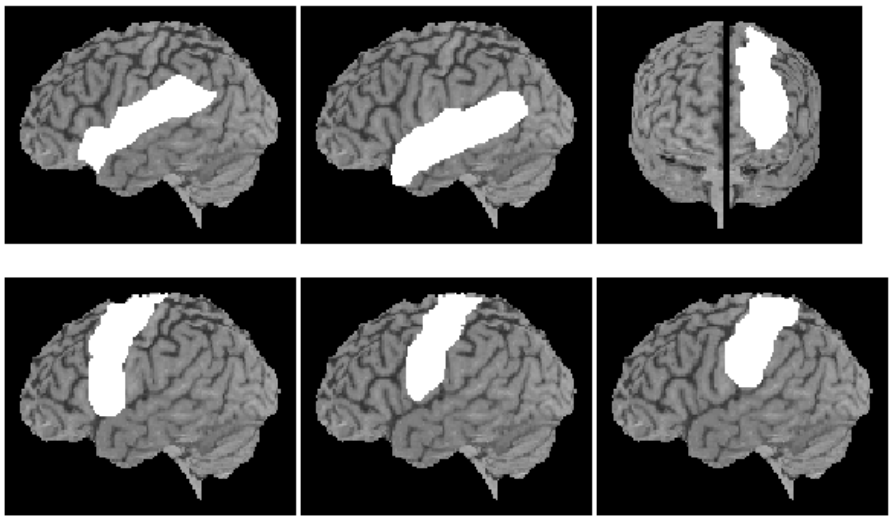

Figure 11 – Examples of search areas built for six major sulci.
From left to right and from top to bottom: lateral, superior temporal, superior frontal, precentral, central, and postcentral sulcus.

2.2.3 Quantitative model of geometry and topology

The third component of the individualized atlas is a statistical model of the cortical topography of each hemisphere. Parameters describe the geometry of each sulcus together with its variability. Other features model the geometrical and topological relations between the different sulci within a same hemisphere, as well as the variability of these relations.

To build such a statistical model, we propose the following method. Firstly, the characteristics of each sulcus curve in the database are computed. The parameters describing the geometry of each sulcus are presented in § 2.2.3.1.

Characteristics modeling the relations between the sulci belonging to a same hemisphere are then computed. The parameters describing relations between sulci are presented in § 2.2.3.2.

A single statistical model can then be built, using both individual and relational parameters. For example, we have, in the same coordinate system, 14 curves corresponding to the right lateral sulcus in different examinations of the database. The length of each curve is computed. The average length and standard deviation on length can then be computed for the right lateral sulcus. The

variation interval for the length of this sulcus can also be computed. The statistical modeling of the different parameters according to their type is described in § 2.2.3.3.

2.2.3.1 Individual characterization of sulci

The parameters of each curve (Figure 6) can be divided into four categories:

Depth: average depth (the average of depth along the sulcus in mm), depth continuity (statistics on depth differences along the sulcus).

Position: starting point position (one of the terminal points of the curve, randomly selected but in a reproducible way for all sulci of the same type), ending point position (the other terminal point), center of gravity position, middle point position.

Continuity: number of interruptions along the curve (in 26-neighborhood), position of the points on either side of the interruption, length of each interruption (in mm), position of the middle of each interruption.

Length and direction: length (sum of the distances between the successive points composing a sulcus in mm), surfacic length (total length minus length of interruptions), the ratio of surfacic length to length, direction vector (normalized vector from starting point to ending point), inertia axis (defined by the center of gravity and the direction vector), orientation continuity (statistics on local orientation variations along the sulcus).

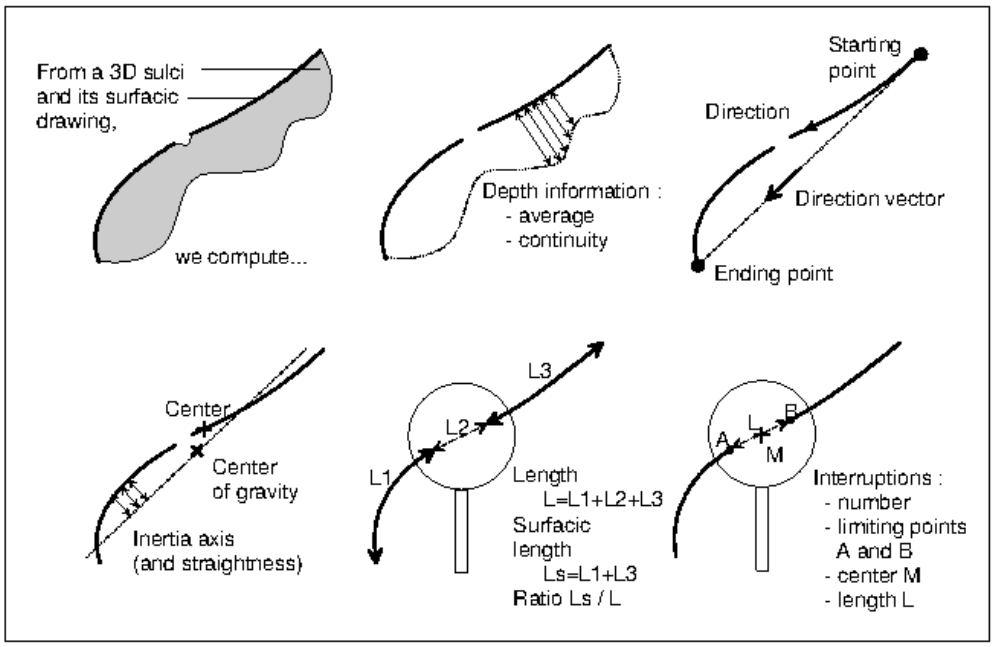

Figure 12 – Major individual parameters of the geometrical and topological model of a sulcus.

2.2.3.2 Relations between sulci

Relations between cortical sulci are very important for their accurate recognition. As a matter of fact, in most paper atlases, a sulcus is represented within its close anatomical neighborhood. Moreover, some sulci are sometimes defined by comparison to others. For instance, the postcentral sulcus can be found a few millimeters backwards the central sulcus (relative position). Another example is the pseudo-parallel course of some sulci, like the precentral, central and postcentral sulci (relative orientation). It should also be noticed that numerous connected sulci can be found in anatomical atlases (connectivity).

The following parameters are computed for each pair of sulci found in the same brain hemisphere of the same image (Figure 7).

Relative position: distance between homologous points (distance in mm between the starting points of a couple of sulci; the same for the ending points, centers of gravity and middle points), vector between two homologous points.

Relative orientation: a relative orientation value, defined as the scalar product between the two normalized main vectors of the two sulci. This parameter has been introduced to quantify the similarity of orientation between sulci, in order to characterize global parallelism between sulci, especially when they are localized in the same neighborhood.

Connectivity: the following parameters are computed only when a couple of sulci are connected. When a connection between two sulci exists, it theoretically involves a single point for each sulcus curve (normally, the anatomical connection should be unique). However, when there are several couples of connected points between two sulci, only one of them is selected: the one who shows the strongest connectivity. If a conflict remains, the couple which includes the nearest point to one of its sulcus extremity is retained. As a matter of fact, in an anatomical point of view, a connection between two sulci can only take place at the extremity of at least one of the sulci.

The parameters modeling a connection between two sulci, computed for each one of the curves, are the following: connectivity point, position from the starting point along the curve (curvilinear abscissa), local orientation (local direction vector of each sulcus in the neighborhood of the connection).

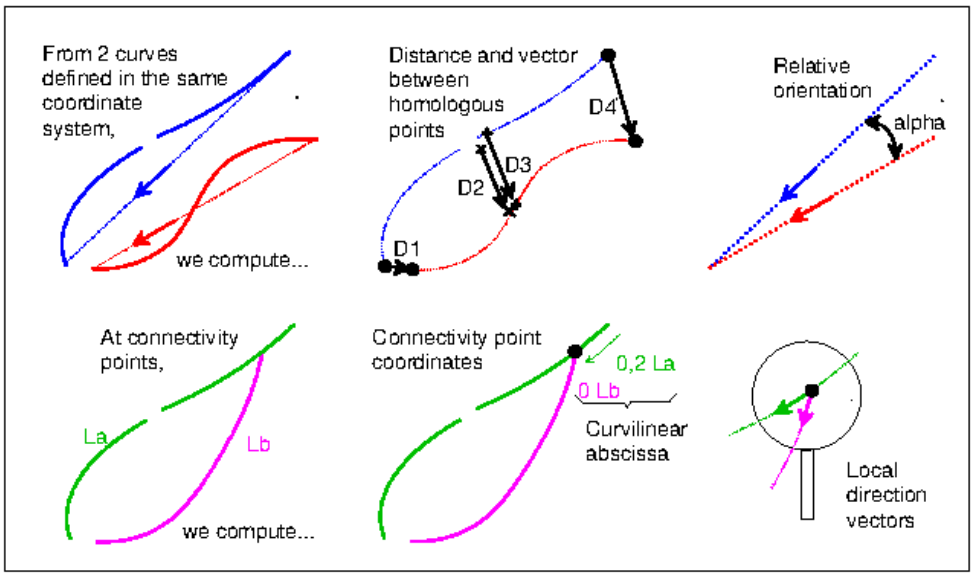

Figure 13 – Model of the geometrical and topological relations between two sulci: major parameters.

2.2.3.3 Building the statistical atlas

From an individual model of each sulcus of the database, a statistical atlas of the whole topography is built for each hemisphere. This a priori model of the sulci to be identified in a particular image (called the "target image") can be considered as a graph where each node is the statistical model of a sulcus, and each edge is the statistical model of the relations between a couple of sulci.

To build this atlas, several parameters must be computed. For each of them (e.g. the length of the right central sulcus), there are as many values as images in the database. From these values, a statistical model of the variations of that parameter in the target image is defined. This model differs according to the parameter type (scalar value, point or vector).

General case: for a scalar value (e.g. the length), the interval of variation is computed (i.e. minimum and maximum) as well as its average and standard deviation. For a point type characteristic, (e.g. the center of gravity), a cloud of points must be modeled. First, the center of gravity of the cloud is calculated, which represents the average localization of the cloud. The

distances between this point and the points belonging to the cloud are then computed, as well as their minimum, maximum, average and standard deviation. For a vector type parameter, (e.g. the vector between centers of gravity), a normalized vector field must be modeled. First, an average vector is computed, which represents the average direction of the field. The angles between this vector and the vectors belonging to the field are then computed, as well as their minimum, maximum, average and standard deviation.

Other cases: the number of interruptions is a scalar piece of information. But, unlike the other data of the same type, it is an integer data. The frequency of interruptions in a sulcus can therefore be computed for each interruption pattern. In the same way, the frequencies of connections are computed for each couple of sulci.

With this process, we get statistical information (Figure 14) that can be compared to those given in the Ono's atlas (Ono et al. 1990), which strongly contributed to the interest and success of this book. The main advantage of our approach is twofold: these data are computed in a completely automatic way, and they can be updated each time a new examination is added to the database.

```
NAME_OF_SULCUS latl (lateral left)

LOCALISATION
origin
        average_point  3 91.597 35.450 21.053
        distance  min 2.1 max 15.2 average 7.5 std_deviation 3.8
(...)

SHAPE_AND_DIRECTION
length  min 105.2 max 142.5 average 122.5 std_deviation 10.8
direction_vector
        average_vector 0.247 0.532 -0.802
        angle  min 1.8 max 9.3 average 6.1 std_deviation 2.4
(...)

CONTINUITY
number_of_interruption(s)  min 0 max 1 average 0.1 (...)
interruption_frequency   0 : 92.86   1 : 7.14
interruption_length  min 2.9 max 2.9 average 2.9 (...)

(...)
RELATIONS_WITH_OTHER_SULCI
sillon centl (central left)
        connectivity
                frequence  21.4
(...)
```

Figure 14 – Example of a text format file (extracts) containing statistical data about a single sulcus and produced by the atlas computation.

2.3 Interindividual normalization

2.3.1 The need for registration

Until now, we have considered a statistical atlas of sulci as a model of a set of curves drawn by an expert and registered in a common coordinate system. But the surfacic part of sulci has been identified in different MR examinations, and the brains belonging to the database have different shapes and sizes. This morphometric variability is very important in an healthy adult population (Figure 15).

	Minimum	Mean	Maximum	St. dev.	diff.max/av.	diff. max/min
Length (mm)	152	170	178	6.03	11%	17%
Height (mm)	107	119	131	5.45	11%	23%
Width (mm)	117	136	146	5.62	14%	24%
Length/width	1.10	1.25	1.36	0.06	12%	23%
Length/height	1.29	1.44	1.58	0.07	11%	23%
Height/width	1.05	1.15	1.37	0.06	19%	30%
Volume (l)	0.93	1.34	1.54	0.13	31%	67%

Figure 15 – Statistics on size and shape variations of 43 in vivo brains observed in 3D MRI. The next to last column shows the maximum difference found between average and minimum or maximum values. The last column shows the difference between minimum and maximum values.

To build a statistical atlas of shape, localization and organization of cortical sulci, sulci are characterized by numerous geometrical and topological parameters (e.g. their length). But it is impossible to compare length from sulci belonging to brains of very different shapes and sizes (Figure 16). It is therefore necessary to beforehand register the curves representing these sulci in a common coordinate system.

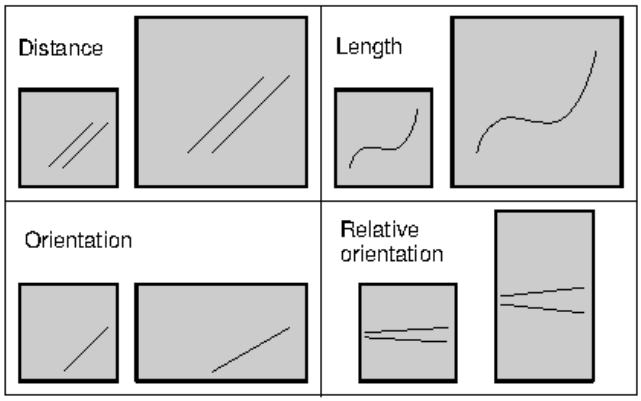

Figure 16 - Influence of shape and size of an object on the geometrical characteristics of its superficial curves.

Let us first examine the choice of the target registration coordinate system. It is useful to remind that the atlas we want to build will further be used to identify sulci in any new MRI. The best coordinate system for registration then clearly appears as the coordinate system of the cerebral examination where the recognition will take place. In this way, the curves are set in a common space and can be statistically processed. But, above all, the computed statistical model of cortical topography will be adapted to the morphological characteristics of the brain under examination. This is a key point of our approach.

2.3.2 Individualized registration

The registration of the database curves towards the brain under examination is performed in two steps. The first one consists in a linear by piece registration. It is intended to grossly superimpose the position and size of the database brains onto those of the target brain. This registration is carried out by the means of the Talairach coordinate system (Talairach and Tournoux 1988) : database sulcus point coordinates are converted into continuous Talairach's coordinate system before being converted again into the target brain image coordinate system. Database sulcus points can then be drawn in the target image. The target image itself is not geometrically transformed (Figure 17). For each sulcus, we get a set of curves which can be seen in the discrete reference system of the target image as a cloud of voxels that extends on all sides of the surface of the hemispheres.

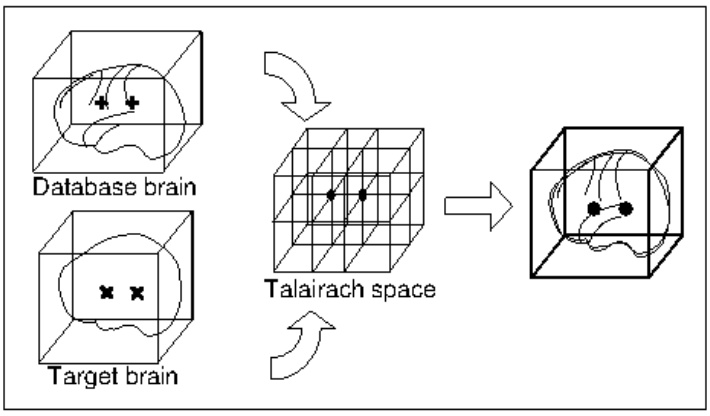

Figure 17 - Principle of registration of the position and dimension of two three-dimensional cerebral images by the Talairach proportional system.

The second step is a nonlinear transformation that takes into account local characteristics of the cerebral surface. This is performed by projecting each point of a database sulcus onto the nearest point of the surface of the target brain, following Euclidean distance (Figure 18). The choice of this very simple projection method can be justified by the fact that the points to be projected are always very close to the hemispherical surface (no more than a few millimeters).

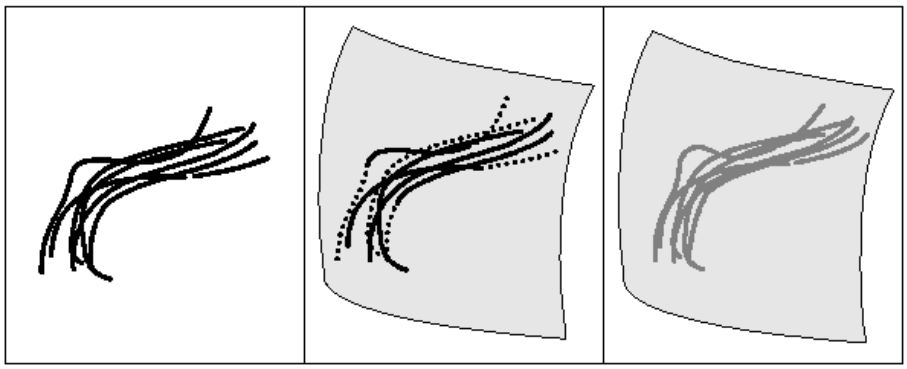

Figure 18 - Principle of the non-linear registration of a set of sulci. After linear registration using the Talairach grid, we get a set of curves for each sulcus (left). The points of these curves are localized on the surface of the hemispheres, but also inside and outside the brain (middle). By projecting them onto the nearest point of surface, we get an area representing the locus of anatomical variation of a sulcus, drawn onto the hemispherical surface of the brain (right).

At the end of these two steps, the curves of the database registered in the target image are located on the surface of the brain in the same way as sulci to be identified. The three components of the atlas adapted to the current image can then be directly extracted. They will then be used at various steps of the identification of sulci. Figure 19 sums up the principle of construction of our statistical and individualized atlas of cortical topography.

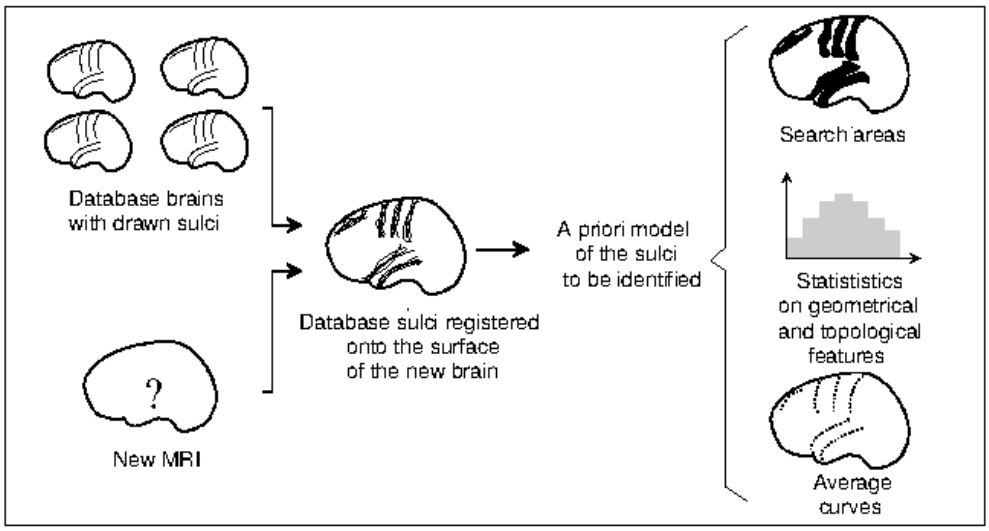

Figure 19 - Principle of construction of the individualized atlas of cortical topography.

3. Results and discussion

3.1 Validation of operators

To validate the principle and implementation of the various operators computing characteristics on sulci, a database of 9 MRI is used, on which the sulci were manually drawn by a medical expert. During manual drawing, the registration step is ignored and statistics are directly computed on the database sulci. Thus, our approach corresponds to the construction process used in most paper atlases. It is the reason why our characteristics can be compared to the data contained in paper atlases, in order to validate the database and its associated operators at the same time. In this paper, results are given for only two characteristics: depth and coefficient of relative orientation.

3.1.1 Depth

The depth of six sulci have been automatically computed for each hemisphere of the 9 brains traced by the expert. Figure 20 shows the average depths for these sulci. They can be compared to information shown in the Ono's atlas (Ono et al. 1990), obtained through the manual post-mortem analysis of 25 brains.

	Ono's atlas		Computed model		Difference (in %)	
	Left	Right	Left	Right	Left	Right
Lateral	28.3	30.4	40.9	37.9	44,5	24,7
Superior temporal	17.4	18.0	18.8	15.1	8	16,1
Precentral	14.1	14.1	15.5	15.6	9,9	10,6
Central	16.0	16.6	16.5	15.6	3,1	6,4
Postcentral	15.7	14.7	16.4	15,4	4,5	4,5
Superior frontal	14.9	14.5	14.9	13,8	0	4,8
			Overall average		11,7	11,2
			Average of the last 5 sulci		5,1	8,5

Figure 20 – Comparison between average depths of twelve sulci (in mm).

Generally, there is a very good correlation between the average depth provided by the atlas and the automatically computed one. Except in the case of the two lateral sulci, only the superior temporal and precentral right sulci present some differences higher than 10%, and this for reasons we have not yet been able to explain. If the lateral sulci are still not taken into account, differences between average measurements in Ono's atlas and ours are as low as 5,1 % for the left hemisphere and 8,5 % for the right hemisphere. This is all the more noticeable since both studies are based on completely different approaches. Thus, our method of depth measurement, although perfectible, can be considered as satisfactory for 10 sulci among 12.

The very significant differences between the values obtained for the lateral sulci and the information provided by Ono's atlas can be mainly due to two reasons. First, the authors of the paper atlas use a particular method to evaluate the depth of the lateral sulcus because of its atypical form. Secondly, our expert has extended the drawing of the lower part of sulci rather far towards the lower part of the brain, and also towards the interhemispheric fissure. It is precisely in this area that coarsest errors occur during depth computation (the plane of calculation being locally directed according to the length of the sulcus and not to its depth). Thus, an adaptation of the process for the lateral sulcus will have to be considered later.

3.1.2 Coefficient of relative orientation

Among the six types of sulci we are studying in both hemispheres, two groups of parallel sulci can be visually distinguished on atlases or on MRI: the lateral sulcus and the temporal superior sulcus on the one hand, and the three "central" sulci (precentral, central, postcentral) on the other hand. Figure 21 allows to verify whether these parallelisms can be found thanks to the coefficient of relative orientation.

		Lateral Sulcus	Superior Temporal s.	Precentral sulcus	Central sulcus	Postcentral sulcus	Superior frontal s.
Lateral Sulcus	G		87 (71 – 98)	22 (1 - 43)	16 (1 - 46)	20 (1 - 43)	83 (76 - 96)
	D		85 (55 – 100)	27 (2 - 53)	24 (1 - 47)	25 (3 - 59)	79 (51 - 100)
Superior Temporal s.	G	87 (71 - 98)		50 (33 - 61)	45 (26 - 65)	50 (21 - 72)	96 (92 - 100)
	D	85 (55 – 100)		48 (21 - 66)	47 (24 - 55)	40 (19 - 62)	94 (80 - 100)
Precentral Sulcus	G	22 (1 - 43)	50 (33 – 61)		97 (82 - 100)	96 (90 - 100)	60 (25 - 77)
	D	27 (2 - 53)	48 (21 – 66)		97 (95 - 100)	93 (82 - 100)	65 (49 - 82)
Central Sulcus	G	16 (1 - 46)	45 (26 – 65)	97 (82 - 100)		97 (90 - 100)	56 (35 - 64)
	D	24 (1 - 47)	47 (24 – 55)	97 (95 - 100)		98 (92 - 100)	63 (45 - 82)
Postcentral sulcus	G	20 (1 - 43)	50 (21 – 72)	96 (90 - 100)	97 (90 - 100)		60 (43 - 87)
	D	25 (3 - 59)	40 (19 – 62)	93 (82 - 100)	98 (92 - 100)		57 (42 - 72)
Superior frontal s.	G	83 (76 – 96)	96 (92 – 100)	60 (25 - 77)	56 (35 - 64)	60 (43 - 87)	
	D	79 (51 – 100)	94 (80 – 100)	65 (49 - 82)	63 (45 - 82)	57 (42 - 72)	

Figure 21 - Table of the coefficients of relative orientation (in percentage): average value, followed by interval of variation (between brackets).

As expected, a strong parallelism can be found between the lateral sulcus and the temporal superior sulcus, with coefficient averages higher than 85% in both hemispheres. In the same way, the expected grouping between the three central sulci can be noticed. In that case, the very good stability of coefficients in the whole database, in particular between the central sulci and the two others, should be emphasized.

But we were also surprised to find a very good correlation between the average directions of the frontal superior and temporal superior sulci (and, to a lesser extent, lateral). It is difficult to detect, because both sulci cannot be simultaneously studied in the same view, owing to their very distant positions, but this correlation is correct. The systematic comparison of sulci features allowed us to update a property the existence of which we did not suspect. The relevance of our model is

confirmed by this observation. Contrary to many other approaches, we chose to characterize the relations between all the elements of cortical topography, and not only relations between adjacent structures. In spite of its simplicity, our characterization method of the relative orientation seems fairly satisfactory.

3.2 Variability and normalization

Space normalization is intended to limit pattern variability. It is often used during the registration of two objects, in order to minimize differences between them, without trying to bring this variation to zero. In the case of cortical sulci, usual registration methods lead to a significant residual variability (Davatzikos 1996, Le Goualher 1997, Sciotte et al. 1996), which cannot be eliminated. When making comparisons between two images, or between an image and an atlas, there must be a common reference space. We use the space of Talairach, associated to a nonlinear projection onto the surface of the brain, with the objective to limit intrinsic variability (Steinmetz et al. 1989).

Three different reference spaces have been compared by measuring residual variability:

- Method 1: the first reference space simply consists of the center of gravity of the brain and distances proportional to the dimensions of the brain according to axes X, Y and Z.
- Method 2: registration in the reference space of Talairach (linear by piece).
- Method 3: registration in the reference space of Talairach, followed by a projection onto the brain surface.

To evaluate the variability of sulci, distances between points of the sulci with the same curvilinear coordinate are measured, as well as the average of these distances. Figure 22 shows the results for each sulcus. The first column is related to the initial variability of the 9 samples of the base, without registration of the sulci, the others correspond to the three previously mentioned methods.

	No registration	Method 1	Method 2	Method 3
Lateral	3.9	3.3	3.2	2.9
Central	4.4	3.6	3.9	3.5
Precentral	4.6	3.9	4.2	3.6
Postcentral	5.2	4.6	4.7	4.6
Superior temporal	5.0	4.1	3.9	3.6
Superior frontal	5.1	4.7	5.0	4.4

Figure 22 - Mean distance (in mm) between sulci.

All three methods reduce residual variability. Globally the linear registration based on the center of gravity of the brain and the registration of Talairach are quite identical. The non-linear method always performs better than the two others. Figure 23 shows projections according to 2 of the 3 axes for the lateral and central sulci.

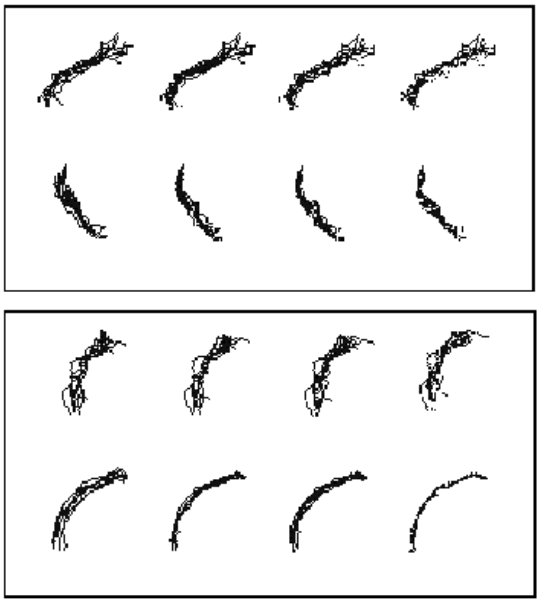

Figure 23 - Sagittal and coronal projection of lateral (top) and central (bottom) sulci. From left to right: no registration, method 1, method 2 and method 3.

This visual assessment confirms numerical results, that is, variability is reduced in all cases but remains relatively high. The modeling of this variability is an essential aspect of the construction of an atlas.

4. Conclusion

Our approach is based on a new method for automatic construction of an atlas of the human cortical sulci from anatomical 3D MRI. This atlas is built from images on which sulci were identified after segmentation, by manually pointing to the segments which compose them. The segmentation is thus respected, without extrapolation due to human operator.

Sulci are represented as 3D curves on the surface of the brain. Depth information is associated to each point of the curves, and gives the distance between the bottom of the sulcus and the surface of the brain. All the points forming the medial surface of a sulcus can then be calculated, in the same manner as in systems working directly on 3D surfaces (Le Goualher et al. 1995, Mangin et al. 1996, Thompson et al. 1996a). Furthermore, our curves are simpler to handle and to visualize.

Our sulcus model includes an average curve which models the shape and the average position of a sulcus. A search area represents the acceptable variability of shape and position. It can be seen as a first approximation of a priori probabilities of presence defined in probabilistic atlases (Thompson et al. 1996b, Le Goualher et al. 1998). In our case, the low number of currently annotated MRI does not allow to calculate significant probabilities. Therefore an alternative approach was considered, corresponding to the thresholding of these probabilities maps. A set of metric characteristics provides usual pattern recognition parameters (length, volume, direction...). The model integrates average values, standard deviation and minimal and maximum values of these measurements. These parameters allow direct comparisons with traditional atlases (Ono et al. 1990) when such measurements are available. A good correlation between the computed values and the values found in atlases has been observed.

To use our atlas for the automatic identification of sulci, it must include information on the existing spatial relations between the various sulci. It is then possible to solve some ambiguities. For instance, two close sulci with similar shapes can be differentiated thanks to their spatial relations. This is included in our approach through connectivity information and metric characteristics defined as vectors and distances between sulci. Unlike other works representing sulci

as graphs, we do not only represent relations of immediate adjacency, but all relations between all sulci of the same hemisphere.

The normalization step is important in order to compare an atlas and an image, or to compare two images. This step is also used to reduce variability between the sulci of several brains when building an average model. Normalization consists in a registration of images in a common reference space. The Talairach reference system is used to perform a linear registration, followed by a projection onto brain surface. Shape and position variability is thus reduced by taking into account local individual deformations. Only residual intrinsic variability, which cannot be eliminated by the registration process, has to be modeled within the atlas.

Until now, our atlas has been used for the identification of six major cortical sulci, giving promising results (Royackkers 1997, Royackkers et al. 1999).

5. References

Bajcsy and Kovacik 1989 R. Bajcsy, S. Kovacik. 1989. Multiresolution elastic matching. *Computer Vision, Graphics and Image Processing*, **46**: 1-21.

Christensen et al. 1995 G.E. Christensen, M.I. Miller, J.L. Marsh, M.W. Vannier. 1995. Automatic analysis of medical images using a deformable textbook. In *Computer Assisted Radiology* (Lemke et al. ed.), pp. 146-151.

Damasio 1995 H. Damasio. 1995. *Human brain anatomy in computerized images*. Oxford university press, New-York.

Davatzikos 1996 C. Davatzikos. 1996. Spatial normalization of 3D brain images using deformable models. *Journal of Computer Assisted Tomography*, **20**(4): 656-665.

Desvignes et al. 1993 M. Desvignes, H. Fawal, M. Revenu, D. Bloyet, P. Allain, J.M. Travère, J.C. Baron. 1993. Calcul de la profondeur en un point des sillons du cortex sur des images RMN tridimensionnelles. *GRETSI, Juan-les-Pins, 1267-1271.*

Evans et al. 1992 A.C. Evans, D.L. Collins, B.Milner. 1992. An MRI-based stereotactic atlas from 250 young normal subjects. *Soc. Neurosci. Abstr.*, **18**: 408-492.

Fawal 1995 H. Fawal. 1995. *Contribution à l'étude d'une base de connaissances adaptées à la définition d'un atlas évolutif du cerveau*. Ph. D Thesis, University of Caen, France.

Fawal et al. 1995 H. Fawal, M. Desvignes, M. Revenu. 1995. Amincissement 3D de surfaces gauches : application à la détection des sillons du cortex cérébral humain. *15ème colloque GRETSI, Juan-les-Pins, France* : 661-664.

Friston et al. 1995 K.J. Friston, J. Ashburner, C.D. Frith, J.B. Poline, J.D. Heather, R.S.J. Frackowiak. 1995. Spatial registration and normalization of images. *Human Brain Mapping*, **2**: 165-189.

Greitz et al. 1991 T. Greitz, C. Bohm, S. Holte, L. Eriksson. 1991. A computerized brain atlas: construction, anatomical content, and some applications. *Journal of Computer Assisted Tomography*, **15**(1) 26-38.

Le Goualher 1997 G. Le Goualher. 1997. *Modélisation de structures anatomiques cérébrales pour l'aide à l'interprétation d'images médicales and à la fusion de données*. Ph. D Thesis, University of Rennes I, France.

Le Goualher et al. 1995 G. Le Goualher, C. Barillot, L. Le Briquer, J.C. Gee, Y. Bizais. 1995. 3D Detection and representation of cortical sulci. In *Computer Assisted Radiology, Springer Verlag, Berlin.*

Le Goualher et al. 1998 G. Le Goualher, E. Procyk, L. Collins, M. Petrides and A.C. Evans. 1998. Sulcus extraction and automatic labelling (SEAL) : Method for mapping of sulcal neuroanatomy. *NeuroImage*, 7(4):S729, 1998.

Mangin et al. 1995 J.F. Mangin, V. Frouin, I. Bloch, J. Régis, J. López-Krahe. 1995. From 3D magnetic resonance images to structural representations of the cortex topography using topology preserving deformations. *Journal of Mathematical Imaging and Vision, 5: 297-318.*

Mangin et al. 1996 J.F. Mangin, V. Frouin, J. Régis, I. Bloch, P. Belin, Y. Samson. 1996. Towards better management of cortical anatomy in multi-modal multi-individual brain studies. *Physica Medica,* **12**(1): 103-107.

Ono et al. 1990 M. Ono, S. Kubik, C.D. Abernathey. 1990. *Atlas of the cerebral sulci*. Georg Thieme Verlag, Stuttgart.

Quinton et al. 1997 O. Quinton, L. Vérard, N. Tzourio, D. Bloyet, J.M. Travère. 1997. Automatic AC-PC identification on 3D T1-MRI using scene analysis. *Neuroimage,* **5**(4): 405.

Royackkers 1997 N. Royackkers. 1997. *Modélisation et reconnaissance des sillons du cortex cérébral humain.* Ph. D Thesis, University of Caen, France.

Royackkers et al. 1999 N. Royackkers, M. Desvignes, M. Revenu. 1999. Une méthode générale de reconnaissance de courbes 3D : application à l'identification de sillons corticaux en imagerie par résonance magnétique. *Traitement du Signal*, **15**(5): 365-379.

Sciotte et al. 1996 N.L. Sciotte, R.P. Woods, J.C. Mazziotta. 1996. Automated image registration using a 105 parameter non-linear model. *Neuroimage,* **3**(3): 123.

Steinmetz et al. 1989 H. Steinmetz, G. Furst, H.S. Freund. 1989. Cerebral cortical localization: application and validation of the proportionnal grid system in MR imaging. *Journal of Computer Assisted Tomography,* **13**(1): 10-19.

Talairach and Tournoux 1988 J. Talairach, P. Tournoux. 1988. *Co-planar stereotaxic atlas of the human brain*. Georg Thieme Verlag, Stuttgart.

Thompson et al. 1996a P. Thompson, C. Schwartz, A.W. Toga. 1996. High-resolution random mesh algorithms for creating a probabilistic 3D surface atlas of the human brain. *Neuroimage,* **3**:19-34.

Thompson et al. 1996b P. Thompson, C. Schwartz, R.T. Lin, A.A. Kahn, A.W. Toga. 1996. Three-dimensional statistical analysis of sulcal variability in the human brain. *The journal of Neuroscience,* **16**(13): 4261-4274.

Thompson and Toga 1996 P. Thompson, A.W. Toga. 1996. Mapping the internal cortex: a probalistic brain atlas based on high-dimensional random fluid transformations. *Neuroimage,* **3**(3): 125.

Tsao and Fu 1981 Y.F. Tsao, K.S. Fu. 1981. A parallel thinning algorithm for 3D pictures. *Computer graphics and image processing*, **17**: 315-331.

Vérard et al. 1997 L. Vérard, P. Allain, J.M. Travère, D.Bloyet. 1997. Fully automatic identification of AC and PC landmarks on brain MRI using scene analysis. *IEEE Transactions on Medical Image Analysis,* **16**(5): 610-616.

6. Acknowledgements

This work is supported by the " Pôle Traitement and Analyse d'Images de Basse-Normandie".